The Influence of the Wind Shears and Sensor Errors upon Aircrafts Landing Process

MIHAI LUNGU
Avionics Department
University of Craiova
107 Decebal Blv., no.6, code: 200440, Craiova
ROMANIA
Lma1312@yahoo.com, mlungu@elth.ucv.ro
http://www.elth.ucv.ro

Abstract: - The paper presents a new system (automatic pilot) for the automatic control of the aircrafts flight altitude in the landing process. The system has two subsystems: the first one controls the altitude of the aircrafts in the glide slope phase of the landing process, while the second subsystem controls the altitude too, but in the flare phase (the second phase of the landing process). The paper author validated the obtained automatic pilot by numerical simulations in Matlab neglecting or taking into consideration the wind shears and sensor errors. He obtained complex Matlab/Simulink models and time characteristics (time variations of the variables involved in the landing process). The wind shears and the sensor errors do not affect the landing process. The most important graphic characteristic is the dependence between the flight altitude and the horizontal displacement.

Key-Words: - Landing process, Dynamic inversion, Sensor errors, Wind shears

1 Introduction

The most difficult task facing a pilot is the aircraft landing. Today, this process is easier because of the electronic technology. The autoland systems were designed to make landing possible in visibility too poor to permit any form of visual landing, although they can be used at any level of visibility [1]. These systems are used when the pilot visibility is less than 600 meters and/or in adverse weather conditions. The pilot must use, in the landing process, an altimeter to determine the aircraft height in a very precise manner in order to start, at the right time, the flare procedure (usually 50 feet above the ground). On aircrafts there are two or three autopilot systems that work in the same time to carry out the landing process, thus providing redundant protection against failures [1].

On aircrafts there is another important system (autopilot): a system for the automatic control of the aircraft lateral movement. This system eliminates or substantially reduces the lateral deviation of the aircraft with respect to the runway line's direction. This system uses an algorithm that elaborates the trajectory command (yaw angular velocity $\dot{\psi}_c$, and the angle ψ_c, respectively) with respect to the tracing error; the imposed roll angle is $\varphi_c = 0$; that is why, the role of the ailerons is only to maintain the aircraft wing in horizontal plane. The system control law is a non-linear one and controls the aircraft so that it follows a plan segment (for example, the runway) whatever the initial conditions (the coordinates and the aircraft direction) are in the case of moderate wind. This law must be modified in the case of strong wind.

The originality of the paper consists of: general design of the new ALS (automatic landing system) including the longitudinal velocity control, the tuning of the PID conventional controllers for the altitude, pitch and velocity channels, the study of the errors induced by the wind shears and errors of the gyro sensors on the proposed ALS.

The paper is organized as follows: the dynamics of the aircraft in longitudinal plane is presented in section 2; in section 3 the author presents the dynamic inversion concept. The description of the automatic control of the flight altitude based on dynamic inversion is given in section 4, while, in section 5, complex simulations have been performed to validate the proposed automatic landing system; finally, some conclusions are shared in section 6.

2 Aircrafts Longitudinal Equations in the Landing Process

For the study of the landing process, the paper

author obtained the dynamic structure from this paper and the validation of this structure is made by simulations in Matlab environment. First of all, the author has to present the model of the longitudinal movement for a Charlie-1 aircraft [2], [3].

The main sensors that are used on aircrafts are: three accelerometers (for the measurement of the accelerations a_x, a_y, a_z, which, by integrating, lead to velocities V_x, V_y, V_z) and three gyrometers (for the measurement of the angular velocities $\omega_x, \omega_y, \omega_z$), connected in an inertial navigation system (INS), sensors for static and dynamic pressure (the first for the determination of the barometric altitude and the both sensors for the determination of the flight velocity), a radio-altimeter or other system for the measurement of the aircraft's height with respect to the ground and so on [4], [5], [6].

The state equation that describes the longitudinal movement of the aircraft is [2], [7], [8]:

$$\dot{\mathbf{x}} = A\mathbf{x} + Bu, \tag{1}$$

with the state vector $\mathbf{x} = \left[V_x \; V_z \; \omega_y \; \theta\right]^T$, the command vector $u = \left[\delta_p \; \delta_T\right]^T, \delta_T$ – the engine command, δ_p – the deflection of the elevator, θ – the pitch angle, $\omega_y = \dot{\theta}$ – the pitch rate, V_x, V_z – the components of the velocity vector $\vec{V}$ with respect to the longitudinal axis of the aircraft (Ox axis) and the vertical one (Oz axis), matrices A and B of form:

$$A = \begin{bmatrix} a_{11} & a_{12} & a_{13} & a_{14} \\ a_{21} & a_{22} & a_{23} & a_{24} \\ a_{31} & a_{32} & a_{33} & a_{34} \\ a_{41} & a_{42} & a_{43} & a_{44} \end{bmatrix} = \begin{bmatrix} X_u & X_w & 0 & -g\cos\theta_0 \\ Z_u & Z_w & V_0 & -g\sin\theta_0 \\ \tilde{N}_u & \tilde{N}_w & \tilde{N}_q & \tilde{N}_\theta \\ 0 & 0 & 1 & 0 \end{bmatrix},$$
$$B = \begin{bmatrix} b_{11} & b_{12} \\ b_{21} & b_{22} \\ b_{31} & b_{32} \\ 0 & 0 \end{bmatrix} = \begin{bmatrix} 0 & X_{\delta_T} \\ Z_{\delta_p} & Z_{\delta_T} \\ \tilde{N}_{\delta_p} & \tilde{N}_{\delta_T} \\ 0 & 0 \end{bmatrix}; \tag{2}$$

the elements $\tilde{N}_u, \tilde{N}_w, \tilde{N}_q, \tilde{N}_\theta, \tilde{N}_{\delta_p}$ are calculated with the formula [9]:

$$\begin{aligned} &\tilde{N}_u = N_u + N_{\dot{w}}Z_u, \tilde{N}_w = N_w + N_{\dot{w}}Z_w, \\ &\tilde{N}_q = N_q + N_{\dot{w}}V_{x0}, \tilde{N}_\theta = -gN_{\dot{w}}\sin\theta_0, \\ &\tilde{N}_{\delta_p} = N_{\delta_p} + N_{\dot{w}}Z_{\delta_p} \end{aligned} \tag{3}$$

with respect to the stability derivates, which, for an aircraft Charlie-1, have the values [3]:

$$\begin{aligned} &X_u = \text{-}0.0238[1/\text{s}], X_w = 0.122[1/s], Z_u = -0.2[1/\text{s}], \\ &Z_w = -0.512[1/\text{s}], N_u = 0.000036[\text{deg/s}\cdot\text{m}], \\ &N_w = -0.006[\text{deg/s}\cdot\text{m}], N_{\dot{w}} = -0.0008[\text{deg/m}], \\ &X_{\delta_T} = 0.1[\text{m/s/deg}], X_{\delta_T} = -1.69\cdot10^{-7}[\text{m/s/deg}], \\ &V_0 = V_{x_0} = 67[\text{m/s}], N_{\delta_T} \cong 0, Z_{\delta_p} = -1.96[\text{m/s/deg}], \\ &N_{\delta_p} = 0, \sin\theta_0 \cong 0, \cos\theta_0 \cong 1. \end{aligned} \tag{4}$$

If one chooses the state vector $\mathbf{x} = \left[V_x \; \alpha \; \omega_y \; \theta\right]^T$, then, in matrices A and B, the second raw changes:

$$\begin{aligned} &Z_u \to Z_u^* = Z_u / V_0, V_0 / V_0 = 1, \\ &-g\sin\theta_0 \to -g\sin\theta_0 / V_0 \cong 0, \\ &b_{21} \to b_{21} / V_0, b_{22} \to b_{22} / V_0. \end{aligned} \tag{5}$$

Thus, the dynamics of the longitudinal movement, for the above mentioned aircraft, is described by the matrices:

$$A = \begin{bmatrix} -0.021 & 0.122 & 0 & -9.69 \\ -0.003 & -0.7535 & 0.91 & 0 \\ 0 & -0.245 & -0.213 & 0 \\ 0 & 0 & 1 & 0 \end{bmatrix}, B = \begin{bmatrix} 0 & 0.1 \\ -0.166 & 0 \\ -1.8 & 0 \\ 0 & 0 \end{bmatrix}. \tag{6}$$

For the landing stage, the values of the longitudinal velocity, at the beginning of the glide slope phase is $V_0 = V_{x_0} = 250[m/s]$, while in the moment when the aircraft begins the flare stage (the second major landing stage, $H = H_0$) it becomes [3]:

$$V_a = V_0 - at_a = V_0 = ct. = 67\,m/s. \tag{7}$$

Because $t_a = 32\,\text{s}$, the distance R from the aircraft to the intersection point of landing path with the runway is obtained using the formula [3]:

$$R = \int_0^t \left(V_a - at\right)\text{d}t; \tag{8}$$

one yields $R \cong 1806\,\text{m}$, while the horizontal covered distance is [2]:

$$x_g = R\cos\left(2.5\cdot\frac{\pi}{180}\right) \cong 1804\,\text{m}. \tag{9}$$

The altitude at which the flare maneuver begins is $H_0 \cong 20\,\text{m}$. Because one has to impose the value of H_0 (the transition altitude from the landing glide slope phase to the flare landing phase), the state vector must contain the variable H (the flight altitude); thus, the equations that describe the longitudinal movement of the aircraft in the landing process are [9]:

$$\begin{aligned}
&\dot{V}_x = X_u V_x + X_w V_z + \tilde{X}_q \omega_y - g\cos\theta_0 \cdot \theta + X_{\delta_p}\delta_p + X_{\delta_T}\delta_T,\\
&\dot{V}_z = Z_u V_x + Z_w V_z + \tilde{Z}_q \omega_y - g\sin\theta_0 \cdot \theta + Z_{\delta_p}\delta_p + Z_{\delta_T}\delta_T,\\
&\dot{\omega}_y = \tilde{N}_u V_x + \tilde{N}_w V_z + \tilde{N}_q \omega_y + \tilde{N}_\theta \theta + N_{\delta_p}\delta_p + N_{\delta_T}\delta_T,\\
&\dot{\theta} = \omega_y,\\
&\dot{H} = V_{x_0}\theta - V_z \Leftrightarrow \dot{H} = V_{x_0}(\theta - \alpha); V_{x_0} = V_0.
\end{aligned} \tag{10}$$

In this case, the state equation is again (1), but the state vector becomes [2]:

$$\mathbf{x} = \begin{bmatrix} V_x & V_z & \omega_y & \theta & H \end{bmatrix}^T \tag{11}$$

and the matrices A and B get the form:

$$A = \begin{bmatrix} a_{11} & a_{12} & a_{13} & a_{14} & 0 \\ a_{21} & a_{22} & a_{23} & a_{24} & 0 \\ a_{31} & a_{32} & a_{33} & a_{34} & 0 \\ 0 & 0 & 1 & 0 & 0 \\ 0 & -1 & 0 & V_0 & 0 \end{bmatrix}, B = \begin{bmatrix} b_{11} & b_{12} \\ b_{21} & b_{22} \\ b_{31} & b_{32} \\ 0 & 0 \\ 0 & 0 \end{bmatrix} \tag{12}$$

or, for the numeric simulation,

$$A = \begin{bmatrix} -0.021 & 0.122 & 0 & -9.69 & 0 \\ -0.003 & -0.7535 & 0.91 & 0 & 0 \\ 0 & -0.245 & -0.213 & 0 & 0 \\ 0 & 0 & 1 & 0 & 0 \\ 0 & -1 & 0 & 67 & 0 \end{bmatrix}, B = \begin{bmatrix} 0 & 0.1 \\ -0.166 & 0 \\ -1.8 & 0 \\ 0 & 0 \\ 0 & 0 \end{bmatrix}. \tag{13}$$

3 Inversion of the Aircrafts Dynamic Model

Flight automatic control structures are based on the dynamic inversion principle [10]. Thus, the linear dynamic model of the aircraft rotation movement is described by equation [2]:

$$\dot{\omega} = A_\omega \omega + A_v V + B\delta_c, \tag{14}$$

with $\omega = \begin{bmatrix} \omega_x & \omega_y & \omega_z \end{bmatrix}^T$ – the vector containing the angular velocities of the aircraft, $V = \begin{bmatrix} V_x & V_y & V_z \end{bmatrix}^T$ – the aircraft translations velocities vector (with its components), $\delta_c = \begin{bmatrix} \delta_p & \delta_e & \delta_d \end{bmatrix}^T$ – the vector containing the command deflection of the elevator (δ_p), the command deflection of the ailerons (δ_e) and the command deflection of the rudder (δ_d); A_ω and A_v – (3×3) matrices that define the rotations and the translations of the aircraft, B – (3×3) invertible input matrix. By dynamic inversion, the control law

$$\delta_c = B^{-1}(\dot{\omega} - A_\omega \omega - A_v V) \tag{15}$$

is obtained.

The author also uses the first differential equation extracted from state equation (1), where $a_{13} = b_{11} = 0$; the two equations are:

$$\dot{\omega}_y = a_{31}V_x + a_{32}V_z + a_{33}\omega_y + b_{21}\delta_p, \tag{16}$$

$$\dot{V}_x = a_{11}V_x + a_{12}V_z + a_{14}\theta + b_{12}\delta_T. \tag{17}$$

It results the equations of the inversed model for the aircraft longitudinal movement:

$$\delta_p = \frac{1}{b_{21}}\left(\dot{\omega}_{y_c} - a_{31}V_x - a_{32}V_z - a_{33}\omega_y\right), \tag{18}$$

$$\delta_T = \frac{1}{b_{12}}\left(\dot{V}_{x_c} - a_{11}V_x - a_{12}V_z - a_{14}\theta\right). \tag{19}$$

For the obtaining of the command inputs of the aircrafts flight automatic control subsystems, one uses a reference model (command filter – low pass filter). The subsystem order, represented by each command filter, is equal with the relative degree of the subsystem model whose output is the state variable commanded by the respective filter output. Thus, for the command of the pitch angle (θ), one uses a filter with the transfer function [2], [11]:

$$\frac{\bar{\theta}(s)}{\theta_c(s)} = \frac{\omega_n^2}{s^2 + 2\xi\omega_n s + \omega_n^2}, \tag{20}$$

with ω_n – the frequency (natural pulsation) and ξ – the damping coefficient. The filter provides the output signals $\bar{\theta}, \dot{\bar{\theta}}, \ddot{\bar{\theta}}$ and, by the integration of $\bar{\theta}$, $\int \bar{\theta}\,dt$ may also be obtained. With these signals the components of the angular acceleration $\ddot{\theta}_c$ may be calculated [12]:

$$\ddot{\theta}_c = \dddot{\bar{\theta}} + k_p^\theta\left(\ddot{\bar{\theta}} - \ddot{\theta}\right) + k_p^{\dot{\theta}}\left(\dot{\bar{\theta}} - \dot{\theta}\right) + k_{pi}^\theta \int\left(\bar{\theta} - \theta\right)dt. \tag{21}$$

For the obtaining of the imposed angular accelerations, the author uses a PID controller (proportional – integral – derivative controller) [11], [13], [14]; the derivative component stabilizes the system with angular velocity steady error equal with zero, the integral component assures the zero steady errors for all the angular variables while the angular acceleration $\dddot{\bar{\theta}}$ leads to faster time responses.

The expression of the imposed angular acceleration $\ddot{\bar{\omega}}_y$ is obtained by the derivation of the equation [9]:

$$\omega_y = \dot{\theta}\cos\varphi + \dot{\psi}\cos\theta\sin\varphi, \tag{22}$$

where $\dot{\omega}_y$ and $\ddot{\theta}$ are replaced by $\overline{\dot{\omega}}_y$ and $\ddot{\theta}_c$; it yields [2]:

$$\dot{\omega}_{y_c} = \ddot{\theta}_c \cos\varphi - \dot{\theta}\dot{\varphi}\sin\varphi + \ddot{\psi}_c \cos\theta \sin\varphi + \\ + \dot{\psi}\left(\dot{\varphi}\cos\theta\cos\varphi - \dot{\theta}\sin\theta\sin\varphi\right). \quad (23)$$

Angular velocity $\ddot{\theta}_c$ from equation (23) is obtained by using equation (21). For the longitudinal movement we have:

$$\dot{\omega}_{y_c} = \ddot{\theta}_c . \quad (24)$$

The velocity V_x is controlled by means of the motor command δ_T using equation (19). The aircraft speed must be constant during the landing process to prevent landing accidents. Taking into account that the relative degree of the aircraft dynamic model with respect to the state variable is 1, the reference model (command filter) must be chosen with the transfer function:

$$\frac{\overline{V}_x(s)}{\overline{V}_{x_c}(s)} = \frac{1}{T_x s + 1}. \quad (25)$$

Because of the slow dynamics of the engine, T_x has large value; for example $T_x = 10^3$ s. The reference model provides signals that are function of $\overline{V}_x$ and $\dot{\overline{V}}_x$. The imposed acceleration is formed using the signal [15]:

$$\dot{V}_{x_c} = \dot{\overline{V}}_x + k_x\left(\overline{V}_x - V_x\right) + k_{xi}\int\left(\overline{V}_x - V_x\right)dt + k_d s\left(\overline{V}_x - V_x\right). \quad (26)$$

Thus, the chosen controller is a PID one. For the longitudinal movement model (13), the author chooses the values [2]:

$$k_x = 20\,s^{-1}, k_{xi} = 0.01 s, k_d = 1.4. \quad (27)$$

At the input of the command filter one applies the signal V_{x_c} (in fact a variation of the velocity V_x); for example, one chooses $\overline{V}_{x_c} = 10$m/s. The time constant is $T_T = 5$ s. The subsystem for the control of the velocity is a part of the system from fig.1 (automatic control system of the aircraft flight in longitudinal plane).

4 Description of the Automatic Control of the Flight Altitude Based on Dynamic Inversion

For the control of the flight altitude H, an exterior loop and an interior loop (for the control of the pitch angle - fig.1) are used. The controller for θ is a PID one – equation (21) with the coefficients [2]:

$$k_p^\theta = 50\left[(\text{deg/s}^2)/\text{deg}\right], \\ k_p^{\dot\theta} = 10\left[(\text{deg/s}^2)/(\text{deg/s})\right], \quad (28) \\ k_{pi}^\theta = 2\left[(\text{deg/s}^2)/(\text{deg}\cdot\text{s})\right].$$

The inverse model is described by equation (18) and the command filter has the form (20), with $\omega_n = 3$ rad/s and $\xi = 0.7$.

For the altitude control, the author uses a PI controller, but, to control the descending velocity $\dot{H}$ too, they choose a PID controller described by equation [16]:

$$\theta_c = k_p^h\left(H_c - H\right) + k_{pi}^h\int\left(H_c - H\right)dt + k_p^{\dot h}\dot{H}_c, \quad (29)$$

where the desired (calculated) descendent velocity is expressed with the formula:

$$\dot{H}_c = V_{x_c}\gamma_c ; \quad (30)$$

γ_c is the imposed (calculated) value of the landing trajectory path; one chooses $\gamma_c = -2.5$ deg. For the model (13), the following values have been chosen:

$$k_p^h = 0.5\,[\text{deg/m}], \\ k_{pi}^h = 10^{-4}\,[\text{deg/m}\cdot\text{s}], \quad (31) \\ k_p^{\dot h} = 0.02.$$

For the calculus of H_c, for the first phase of the landing process $(H \geq H_0)$, one uses equation:

$$H_c = \left(x - x_{p_0}\right)\cdot\tan(\gamma_c),\ H \geq H_0 . \quad (32)$$

For an instantaneous point $A_p\left(x_p, H_p\right)$, the above equation is equivalent with the following one:

$$x_{p_0} = x_p - H_p / \tan(\gamma_c). \quad (33)$$

So, for the glide slope phase of the landing process, the equation (32) is used, with x_{p_0} of form (33) and with $\gamma_c = -2.5$ deg. For the flare process $(H < H_0)$, the expression of H_c is:

$$H_c = H_0 \cdot \exp\left(-\frac{t - t_0}{\tau}\right),\ H_0 = H(t_0), \quad (34)$$

t_0 being the moment when the aircraft passes from the glide slope phase to the flare stage. Taking into account that:

$$t - t_0 = \frac{x - x_0}{\dot{x}}, \qquad (35)$$

the equation (34) becomes:

$$H_c = H_0 \cdot \exp\left(-\frac{x - x_0}{\tau \cdot \dot{x}}\right), H < H_0 . \qquad (36)$$

For the studied example, $\tau = 8\,\text{s}$ and $T_p = 0.1\,\text{s}$.

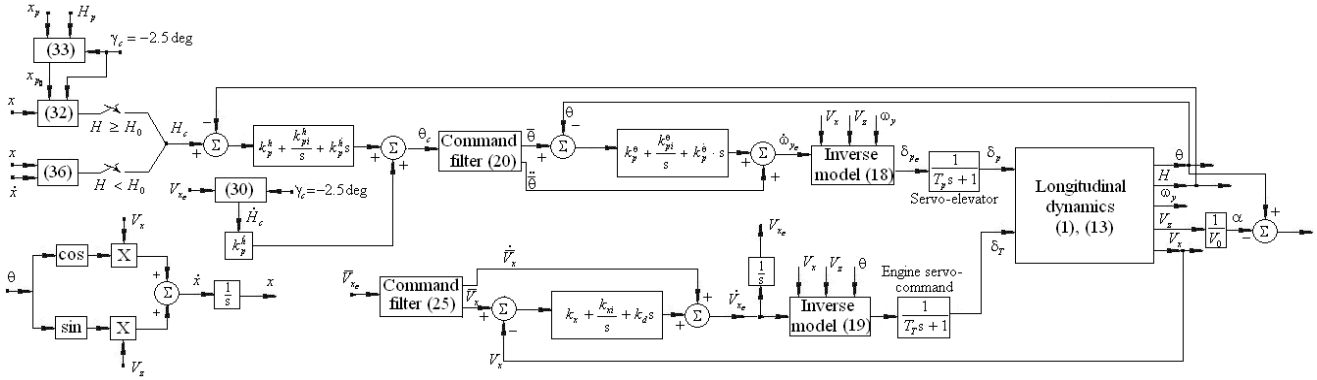

Fig.1 Aircrafts automatic control system for the landing process in the longitudinal plane

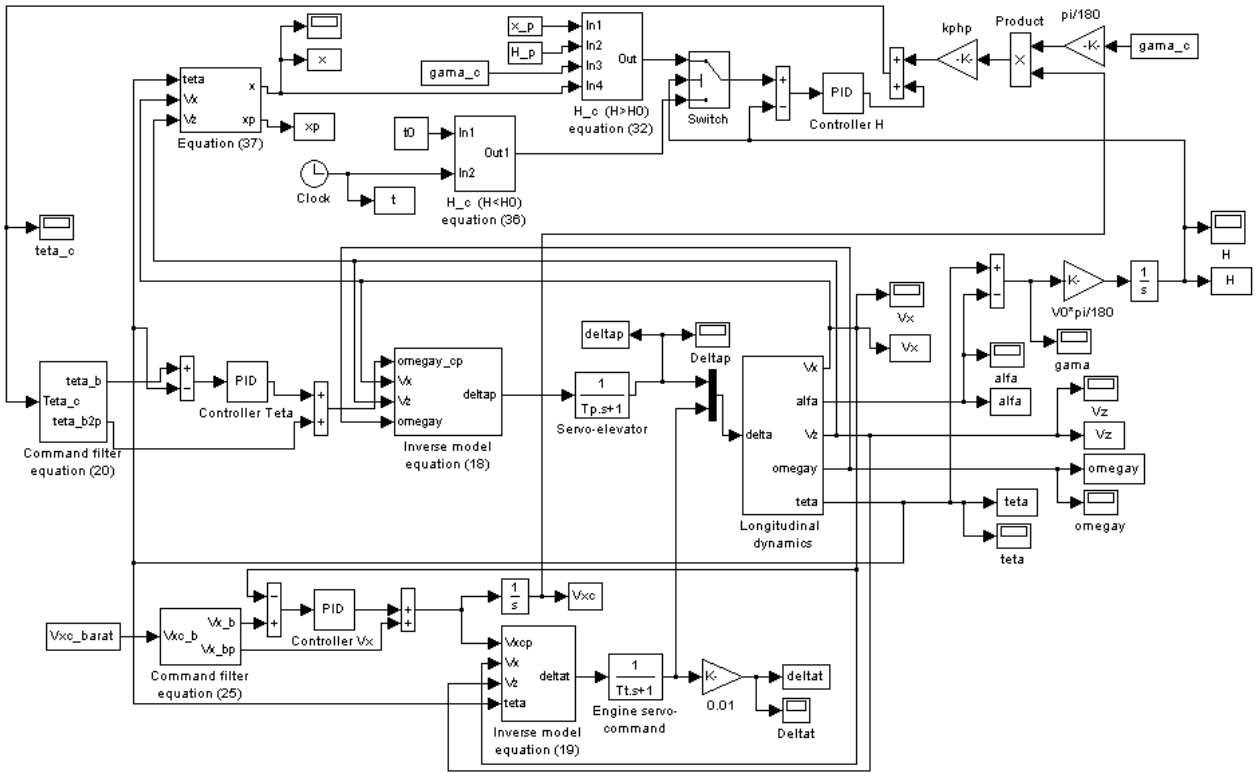

Fig.2 The Matlab/Simulink model for the block diagram from fig.1

The horizontal displacement velocity is calculated with [2]:

$$\dot{x} = V_x \cos\theta + V_z \sin\theta . \qquad (37)$$

In fig.1 the author presents the aircrafts automatic control system for the landing process in the longitudinal plane.

5 Computer Simulations

If the wind shears are taken into consideration, the aircraft dynamics change. The linear model of the aircraft movement, in longitudinal plane, becomes:

$$\dot{\mathbf{x}} = A\mathbf{x} + Bu + B_v v_v , \qquad (38)$$

with $\mathbf{x}$ - the state vector, u – the command vector, v_v – the disturbances vector (the components of the wind velocity on aircraft axes Ox and Oz),

$$\begin{aligned} \mathbf{x} &= \left[V_x \;\; \alpha \;\; \omega_y \;\; \theta\right]^T, \\ u &= \left[\delta_p \;\; \delta_T\right]^T, \\ v_v &= \left[V_{vx} \;\; V_{vz}\right]^T, \end{aligned} \tag{39}$$

$$\begin{aligned} B_v &= \begin{bmatrix} -a_{11} & -a_{21} & -a_{31} & 0 \\ -a'_{12} & -a'_{22} & -a'_{32} & 0 \end{bmatrix}^T; \\ B_v &= \begin{bmatrix} -a_{11} & -a_{21} & -a_{31} & 0 \\ -a_{12}/57.3V_0 & -a_{22}/57.3V_0 & -a_{32}/57.3V_0 & 0 \end{bmatrix}^T; \end{aligned} \tag{40}$$

the elements of the matrix B_v are calculated with equations from [9], with respect to the stability derivates for the aircraft type.

The calculus equations for the components of the wind velocity may be of forms [17], [18]:

$$\begin{aligned} V_{vx} &= -V_{vx_0} \sin(\omega_0 t), \\ V_{vz} &= -V_{vz_0}\left[1 - \cos(\omega_0 t)\right], \\ \omega_0 &= 2\pi / T_0 . \end{aligned} \tag{41}$$

In fig.2, one presents the Matlab/Simulink model for the block diagram from fig.1. This Matlab/Simulink model has 8 subsystems: "Command filter equation (20)" – fig.3, "Equation (37)" - fig.4, "H_c (H>H0) equation (32)" – fig.5, "H_c (H<H0) equation (36)" – fig.6, "Inverse model equation (18)" – fig.7, "Longitudinal dynamics" – fig.8, "Command filter equation (25)" – fig.9, "Inverse model equation (19)" – fig.10.

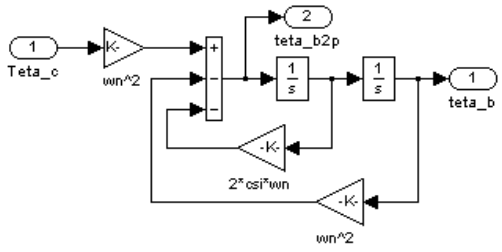

Fig.3 The Matlab/Simulink model for the subsystem "Command filter equation (20)"

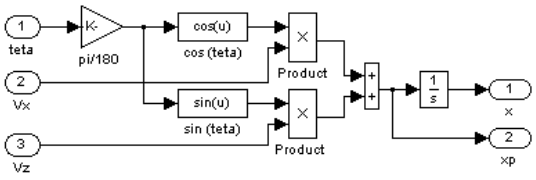

Fig.4 The Matlab/Simulink model for the subsystem "Equation (37)"

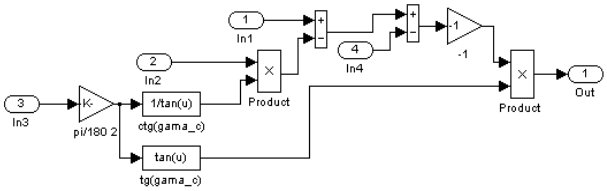

Fig.5 The Matlab/Simulink model for the subsystem "H_c (H>H0) equation (32)"

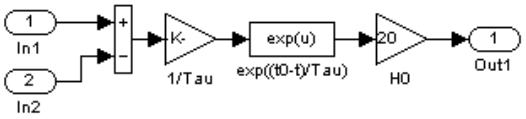

Fig.6 The Matlab/Simulink model for the subsystem "H_c (H<H0) equation (36)"

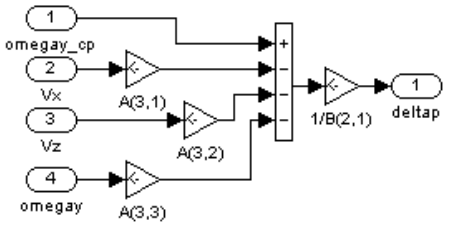

Fig.7 The Matlab/Simulink model for the subsystem "Inverse model equation (18)"

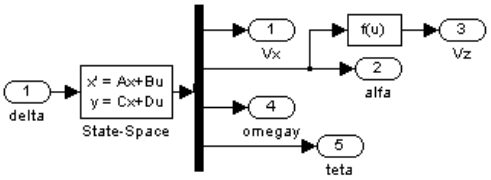

Fig.8 The Matlab/Simulink model for the subsystem "Longitudinal dynamics"

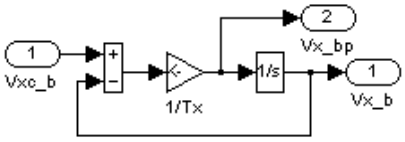

Fig.9 The Matlab/Simulink model for the subsystem "Command filter equation (25)"

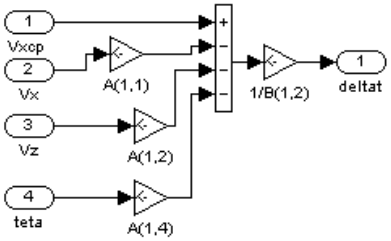

Fig.10 The Matlab/Simulink model for the subsystem "Inverse model equation (19)"

By the simulation of the Matlab/Simulink model from fig.2, the author obtained the time characteristics from fig.11, fig.12 and fig.13. In fig.11 the author presents the time variations of $\alpha, \gamma, \omega_y, V_x, V_z, \theta, \delta_p, \delta_T$ and H for the first phase of the landing process – the glide slope phase. The characteristics with blue solid line correspond to the case when the landing process is not affected by the wind shears (the wind velocity is neglected). The characteristics with red dashed line correspond to the landing process affected by wind shears. Same characteristics, but for the second phase of the landing process – the flare phase, are presented in fig.12.

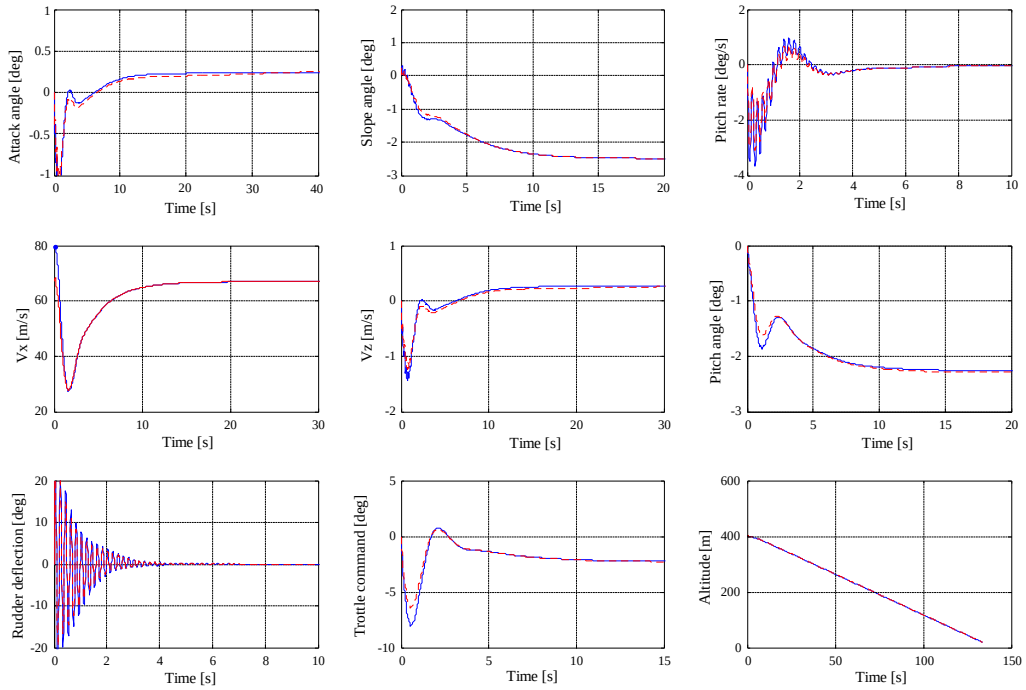

Fig.11 Time variations of the landing process variables in the first phase – glide slope phase

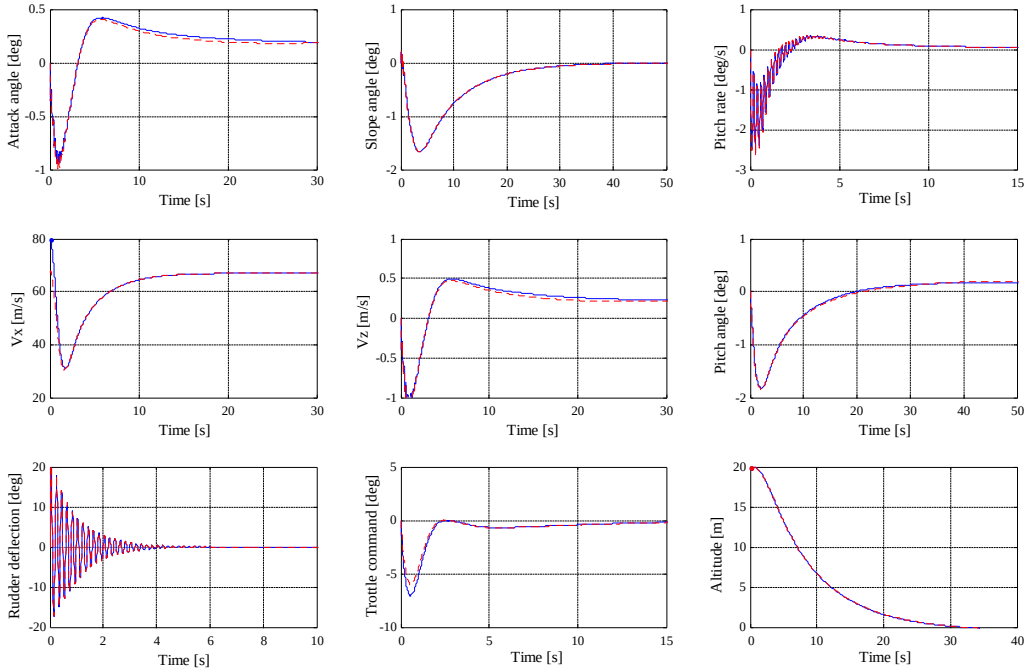

Fig.12 Time variations of the landing process variables in the second phase – flare phase

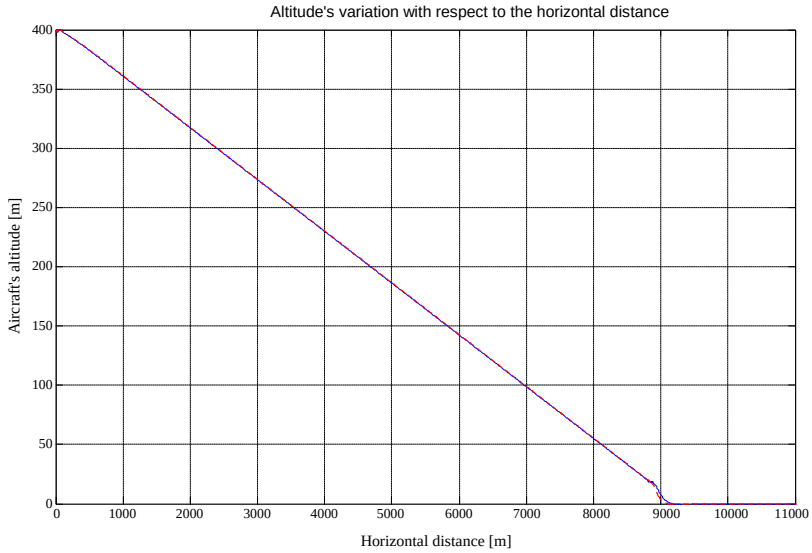

Fig.13 The time variation of the flight altitude for the entire landing process

In fig.13 one presents the variation of the altitude H with respect to the horizontal displacement x for the whole landing process (blue solid line for the case "without wind" and red dashed line for the case "with wind"). As one can see, the variation of altitude in the glide slope phase is linear, while, in the flare phase, the altitude descends aperiodically and tends to zero. Time variations of the altitude can also be seen in the last graphic from fig.11 (glide slope phase) and fig.12 (flare phase).

The wind with the components (41) does not disturb the landing process. Thus, the automatic pilot from fig.1 is a robust one, with good results.

For the obtaining of the graphics in fig.11 and fig.12, the Matlab/Simulink model in fig.2 has been used. Because the landing process has two important phases, the system in fig.1 has 2 important subsystems: the system for the automatic control of the flight altitude in the glide slope phase and the system for the automatic control of the flight altitude in the flare phase. The graphics in fig.11 have been obtained by using the first subsystem, while the graphics in fig.12 have been obtained by using the second subsystem.

The Matlab/Simulink models of the two subsystems are presented in fig.14 and fig.15.

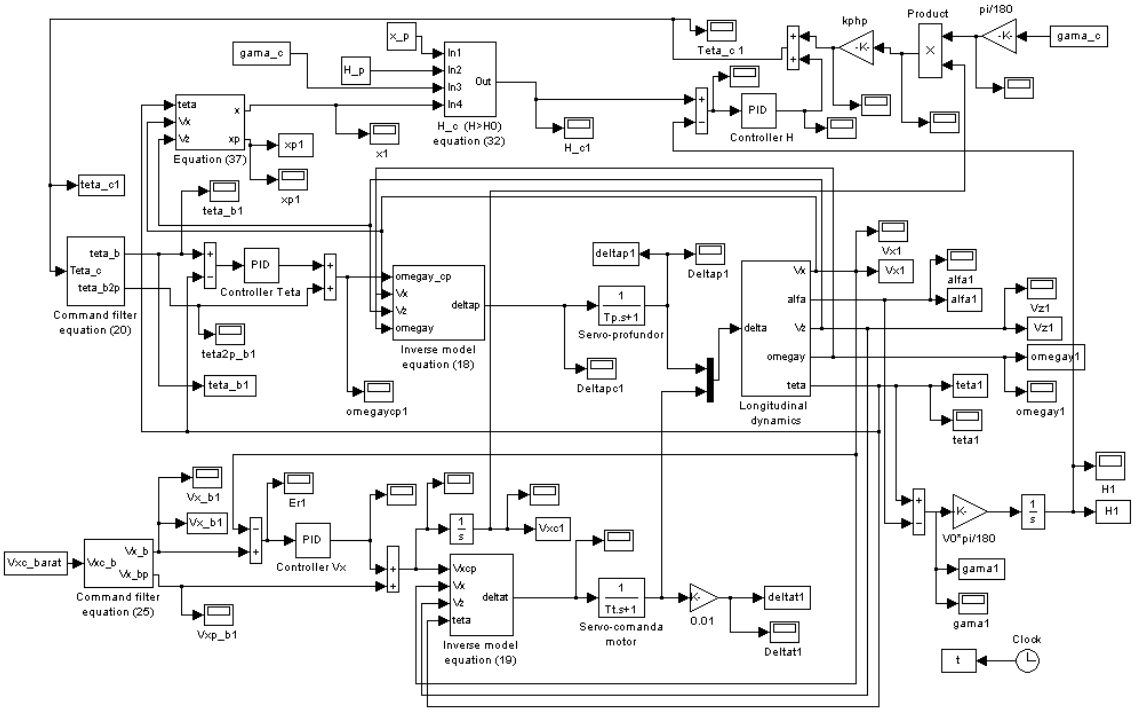

Fig.14 The Matlab/Simulink model for the automatic control of the flight altitude in the glide slope phase

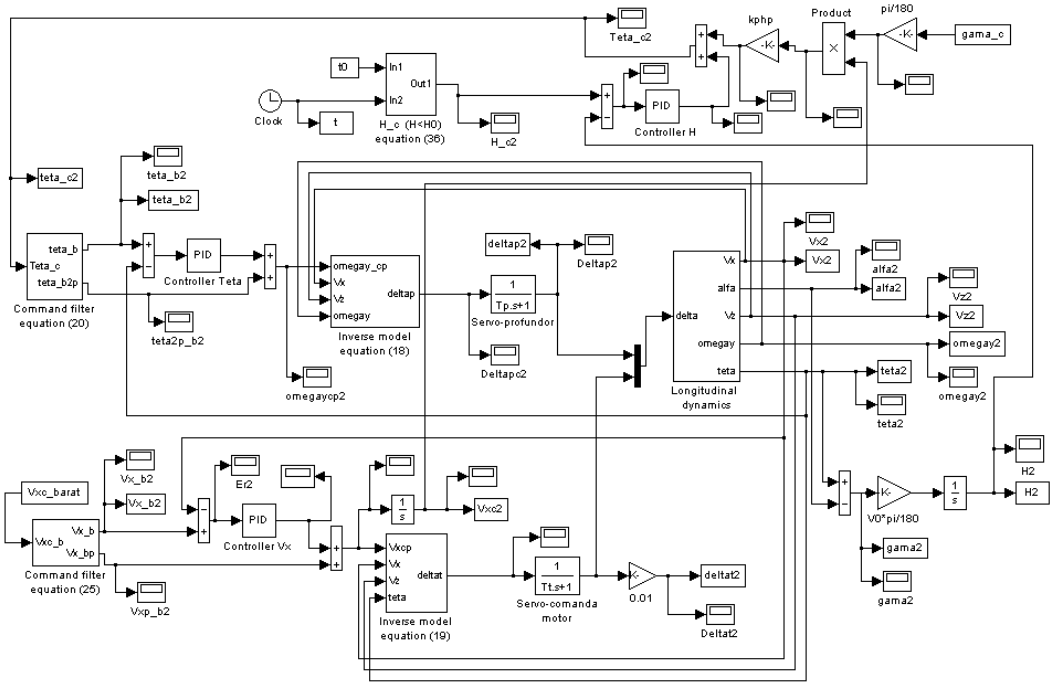

Fig.15 The Matlab/Simulink model for the automatic control of the flight altitude in the flare phase

In the above simulations one did not take into consideration the errors of the sensors (used for the measurement of the state variables). These errors are considered in simulations below.

For the determination of the pitch angle θ one may use an integrator gyro. This gyro has errors and it is interesting to see if the sensor errors affect the landing process. One considers the error model that takes into account the parameters from the data sheets offered by the sensors producers; the error model is described by the equation:

$$\theta = (\theta_i + S \cdot a_r + B + \nu)\left(1 + \frac{\Delta K}{K}\right), \qquad (42)$$

where θ is the output pitch angle (the perturbed signal), θ_i – the input pitch angle, S – the sensibility to the acceleration a_r applied on an arbitrary direction, B – the bias, K – the scale factor, ΔK – the calibration error of the scale factor and ν – the sensor noise.

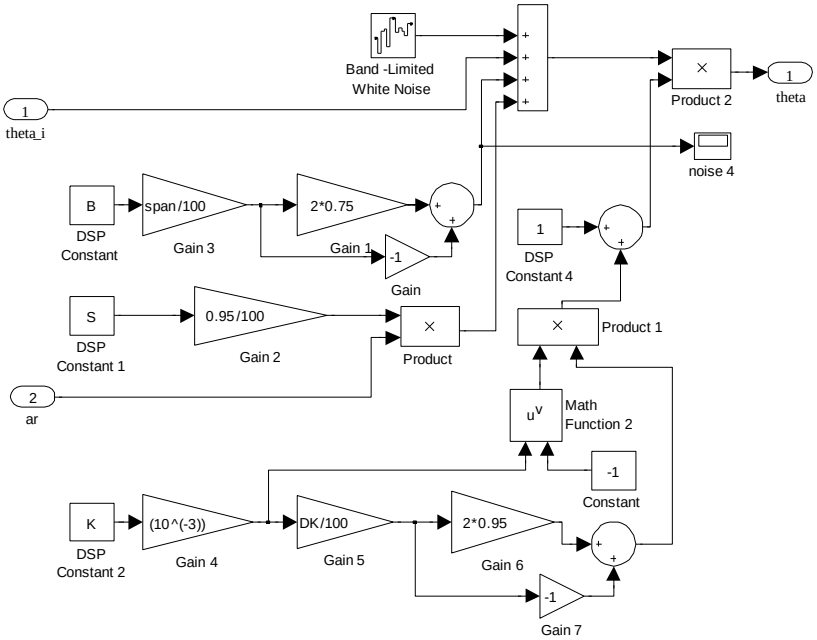

Fig.16 Matlab/Simulink model for the gyro sensor

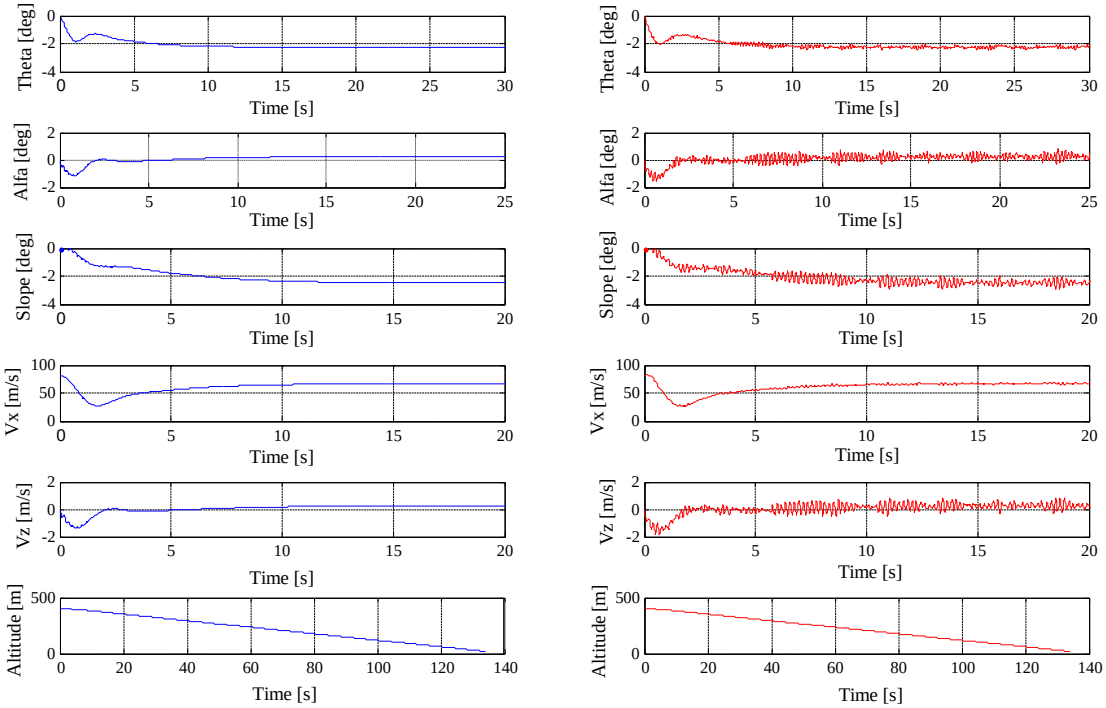

Fig.17 The influence of sensor errors in the glide slope phase of the landing process

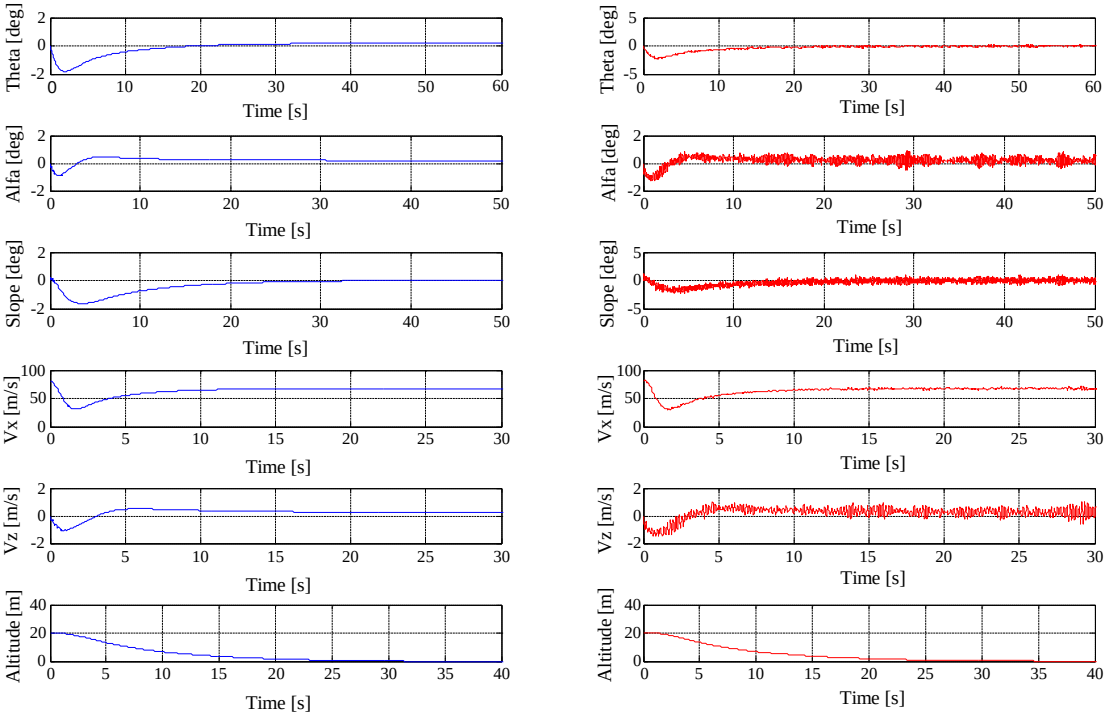

Fig.18 The influence of sensor errors in the flare phase of the landing process

A Matlab/Simulink model (fig.16) has been introduced in the model from fig.2 in the feedback after the pitch angle θ.

The bias is given by its maximum value B as percentage of span, the calibration error of the scale factor is given by its absolute maximum value ΔK as percentage of K, while the noise is given using its maximum density value. Using the Matlab function "rand(1)" one generates the bias, by a random value in the interval $(-B, B)$, the sensibility S to acceleration a_r, applied on an arbitrary direction in the interval $(0, S)$ and the calibration error of the scale factor in the interval $(-\Delta K, \Delta K)$. The noise is generated by means of a

Simulink block "Band-Limited White Noise" using the Matlab function "RandSeed" generating a random value of its density in the interval $(80\% \cdot \nu_d,\ \nu_d)$.

The inputs of the error model are the pitch angle θ_i and the acceleration a_r, considered to be the resultant acceleration signal that acts upon the carry vehicle, while the output is the disturbed pitch angle θ. In the numerical simulation, the following sensor parameters have been used: the noise density - $0.1\left[\text{deg}/\sqrt{Hz}\right]$, the bias - $5\left[\text{deg}\right]$, the error of the scale factor - $1\% \cdot K$, the sensibility to accelerations - $0.18\left[\text{deg}/\ g\right]$; $\bar{g}$ is the gravitation acceleration.

The influences of the sensor errors in the glide slope phase of the landing process is presented in fig.17, while the influences of the sensor errors in the flare phase of the landing process is presented in fig.18. Although the errors of the gyro sensor (for the measurement of the pitch angle) affect most of the variables, the time variation of the altitude and the time length of the landing process phases are not affected. So, the author concludes that the sensor errors do not affect the landing process.

6 Conclusion

The new system (automatic pilot) presented in this paper may be used, with good results, to the automatic control of the aircrafts flight altitude in the landing process. The system has two subsystems: the first one controls the altitude of the aircrafts in the glide slope phase of the landing process, while the second subsystem controls the altitude too, but in the second phase of the landing process (flare phase).

The paper author validated the obtained automatic pilot by numerical simulations in Matlab/Simulink environment; he obtained a lot of time characteristics (time variations of the variables involved in the landing process) in the presence or in the absence of wind shears. The wind with the components (41) does not disturb the landing process, the automatic pilot from fig.1 being a robust one.

Interesting results have also been obtained taking into account the sensor errors (the bias, the scale factor, the calibration error of the scale factor and the sensor noise). Although the errors of the gyros sensor (for the pitch angle measurement) affect most of the variables, the time variation of the altitude and the time length of the landing process phases are not affected. So, the author concludes that the sensor errors do not affect the landing process.

The variation of altitude in the glide slope phase is linear, while, in the flare phase, the altitude descends aperiodically and tends to zero. The author intends in the future to project an automatic pilot, based on dynamic inversion too, for the lateral movement of the aircrafts.

7 Acknowledgments

This work was supported by the strategic grant POSDRU/89/1.5/S/61968 (2009), co-financed by the European Social Fund within the Sectorial Operational Program Human Resources Development 2007 - 2013.

References:

[1] http://en.wikipedia.org/wiki/ Automatic landing systems

[2] Lungu M., Mastorakis N., Grigorie L., Automat Control of the Flight Altitude Using the Dynamic Inversion and the Influence of Wind Shears and Sensors' Errors on the Aircrafts' Landing Process. *7th WSEAS International Conference on Dynamical Systems and Control* 1–3 July, 2011, Iasi, Romania; vol. pp. 97-104.

[3] Donald Mc.L., *Automatic Flight Control Systems.* Prentice Hall Publisher, 1990, 593 pp.

[4] Ricny V., Mikulec J., Measuring flying object velocity with CCD sensor". *IEEE Aerospace and Electronic Systems Magazine*, vol.9, Issue 6, pp. 3-6, June 1994.

[5] Gollomp B., The angle of attack. *IEEE Instrumentation & Measurement Magazine*, vol.4, Issue 1, pp. 57-58, 2001.

[6] Chelaru T.V., Pana V., Stability and Control of the UAV Formations Flight. *WSEAS Transactions on Systems and Control*, Issue 1, Vol. 5, January 2010.

[7] Carlos M., Vélez S., Andrés A., Multirate control of an unmanned aerial vehicle, *WSEAS Transactions on Circuits and Systems* Issue 11, Volume 4, November 2005, ISSN 1109 – 2734.

[8] Ching-Hung Lee, Bo-Ren Chung, FNN-based Disturbance Observer Controller Design for Nonlinear Uncertain Systems. *WSEAS Transactions on systems and control,* Vol. 2, March 2007.

[9] Lungu M., *Sisteme de conducere a zborului.* Sitech Publisher, 2008.

[10] Mackunis P.M., Patre M.K., Kaise W.E. Dixon W., Asymptotic Tracking for Aircraft via Robust and Adaptive Dynamic Inversion Methods, *IEEE Transactions on Control Systems and Technology*, vol. 18, no.6, 2010.

[11] Yasemin I., Pitch Rate Damping of an Aircraft by Fuzzy and Classical PD Controller. *WSEAS Transactions on Systems and Control*, Issue 7, vol. 5, July 2010.

[12] Calise, A.J., Rysdyk R.T., Adaptive Model Inversion Flight Control for Tiltrotor Aircraft, *AIAA Guidance, Navigation and Control,* vol. 22, pp. 402-407, 1999.

[13] Huang C., Shao Q., Jin P., Zhu Z., Luoyang P., Pitch Attitude Controller Design and Simulation for a Small Unmanned Aerial Vehicle. *International Conference on Intelligent Human-Machine Systems and Cybernetics, IHMSC '09*, Hangzhou, Zhejiang, 26-27 Aug. 2009, pp. 58-61.

[14] Santos S., Oliveira N., Test platform to pitch angle using hardware in loop. *39th IEEE Frontiers in Education Conference, FIE '09*, San Antonio, 18-21 Oct. 2009, pp. 1-5.

[15] Kargin V., *Design of An Autonomous Landing Control Algorithm for A Fixed Wing UAV*. MS Thesys, Middle East Technical University, Ankara, Turkey, 2007.

[16] Pashilkar A.A. Sundararajan N., Saratchandran P.A., Fault-Tolerant Neural Aided Controller for Aircraft Auto-Landing. *Aerospace Science and Technology*, vol.10, Issue 1. 2006, pp. 49-61.

[17] Che J., Chen D., Automatic Control using H_∞ Control and Stable Inversion. *Proceedings of the 40th IEEE Conference on Decision and Control*, Orlando, Florida, USA, 2011, pp. 241–246.

[18] Kang W., Idiori A., Flight Control in a Wind shear via Nonlinear H_∞ Methods. *Proceedings of the 31th Conference on Decision and Control*, Orlando, Florida, USA, 2011, pp. 1135–1142.